XII International Conference on Computational Plasticity. Fundamentals and Applications
COMPLAS XII
E. Oñate, D.R.J. Owen, D. Peric and B. Suárez (Eds)

ANALYSIS OF ULTRA LOW CYCLE FATIGUE PROBLEMS WITH THE BARCELONA PLASTIC DAMAGE MODEL

X. MARTINEZ[*†] , S. OLLER[*◊] , L.G. BARBU[*◊] AND A.H. BARBAT[*◊]

[*] International Center for Numerical Methods in Engineering (CIMNE)
Universidad Politécnica de Cataluña
Campus Norte UPC, 08034 Barcelona, Spain
e-mail: x.martinez@upc.edu

[†] Departament de Ciència i Enginyeria Nàutiques, UPC
[◊] Departament de Resistència de Materials i Estructures a l'Enginyeria, UPC

Key words: Ultra low cycle fatigue, plastic damage, isotropic and kinematic hardening.

Abstract. This paper presents a plastic formulation based on the Barcelona plastic damage model ([1], [2]) capable of predicting the material failure due to Ultra Low Cycle Fatigue. This is achieved taking into account the fracture energy dissipated during the cyclic process. This approach allows the simulation of ULCF in regular cyclic tests, but also in non-regular cases such as seismic loads.

1 INTRODUCTION

Ultra Low Cycle Fatigue (ULCF) takes place for a reduced number of cycles, usually less than 1000 and often less than 100. Contrary to what occurs with high cycle fatigue, in this failure mechanism plasticity plays an important role. The most common procedures used to simulate ULCF are those based on counting the number of cycles that can be applied to the material for a given plastic strain. Examples of those approaches are the Coffin-Manson rule [3], the Basquin rule [3], or the enhanced rule proposed by Xue in [4]. However, one of the main drawbacks of these formulations is that they require of regular cycles to predict the material failure, and often this regularity does not exist. An example of an ULCF failure due to an irregular cyclic load is found in the failure of large diameter pipes subjected to seismic loads, where the frequency varies along time and each cycle may have different amplitude.

Current work proposes the use of a plastic damage model to simulate Ultra Low Cycle Fatigue. The model developed is based in the Barcelona model originally formulated by Lubliner et al. [1]. Although this model was originally developed for concrete, here is presented a new kinematic and isotropic hardening law specifically defined for the simulation of steel. One of the main characteristics of the model is that the hardening behaviour of the material is driven by the plastic energy dissipated. With this approach, it is possible to measure the energy required in each hysteresis cycle, as well as the available energy remaining on the material. Failure takes place when all the plastic fracture energy of the material has been dissipated.

This paper shows that with the proposed model it is possible to simulate an ULCF failure

by calibrating the available plastic energy of the material. One of the main advantages of the proposed procedure is that it is capable of predicting the material failure independently of the number of cycles applied to the structure, as well as the amplitude and frequency of those cycles. This is because the model is based on the actual loading history of the structure, being this loading history as random as needed. Therefore, it is possible to simulate the material failure produced by ULCF in a seismic event, or on any other cyclic load scenario. Besides, the formulation is capable of using any yield and potential surfaces to characterize the material, which increases its applicability to different steel alloys.

2 PLASTIC DAMAGE MODEL

This work will not describe the complete plastic damage model, as it can be obtained from reference [1]. Instead, it will focus on the elements that differentiate current model from the Barcelona model proposed by Lubliner *et al.*

The inelastic theory of plasticity can simulate the material behavior beyond the elastic range, taking into account the change in the strength of the material through the movement of the yield surface, isotropic and kinematic. It is assumed that each point of the solid follows a thermo-elasto-plastic constitutive law (stiffness hardening/softening) ([1], [5] and [6]) with the stress evolution depending on the free strain variable and plastic internal variables.

The yield surface is defined by a function F that accounts for the residual strength of the material, which depends on the current stress state, the temperature and the plastic internal variables. This F function has the following form, taking into account isotropic and kinematic plastic hardening (Bauschinger effect [7]),

$$F(S_{ij},\gamma^p,\theta) = f(S_{ij}-\alpha_{ij}) - K(S_{ij},\kappa^p,\theta) \le 0 \qquad (1)$$

where $f(S_{ij}-\alpha_{ij})$ is the uniaxial equivalent stress functions depending of the current value of the stresses S_{ij}, α_{ij} the kinematic plastic hardening internal variable, $K(S_{ij},\kappa^p,\theta)$ is the plastic strength threshold, κ^p is the plastic isotropic hardening internal variable, and θ is the temperature at current time t ([1], [5] and [6]).

2.1 Kinematic Hardening

Kinematic hardening accounts for a translation of the yield function and allows the representation of the Bauschinger effect in the case of cyclic loading. A two dimensional representation of this movement in the plane $S_1 - S_2$ is shown in the following figure:

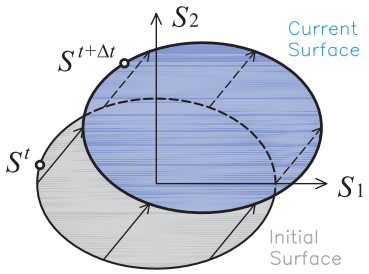

Figure 1. Translation of the yield surface result of kinematic hardening

This translation is driven by the kinematic hardening internal variable α_{ij} which, in a general case, varies proportionally to the plastic strain of the material point [7]. There are several laws that define the evolution of this parameter. Current work uses a non-linear kinematic hardening law, which can be written as:

$$\dot{\alpha}_{ij} = c_k \dot{E}^p_{ij} - d_k \alpha_{ij} \dot{p} \tag{2}$$

Where c_k and d_k are material constants, E^p_{ij} is the plastic strain, and $\dot{p}$ is the increment of accumulative plastic strain, which can be computed as: $\dot{p} = \sqrt{2/3 \cdot \dot{E}^p_{ij} : \dot{E}^p_{kl}}$.

2.2 Isotropic Hardening

Isotropic hardening provides an expansion or a contraction of the yield surface. The expansion corresponds to hardening and the contraction to a softening behavior. In the following figure is depicted a two dimensional representation of this effect in the plane $S_1 - S_2$:

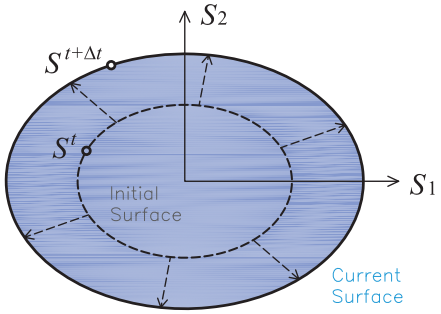

Figure 2. Expansion of the yield surface result of isotropic hardening

The evolution of isotropic hardening is controlled by the evolution of the plastic hardening function K, which is often defined by an internal variable κ^p. The rate equation for these two functions may be defined, respectively:

$$\dot{K} = \dot{\lambda} \cdot H_k = h_k \cdot \dot{\kappa}^p \tag{3}$$

$$\dot{\kappa}^p = \dot{\lambda} \cdot H_k = \dot{\lambda} \cdot \left[h_k : \frac{\partial G}{\partial S} \right] = h_k \cdot \dot{E}^p$$

where k denotes scalar and $\mathbf{k}$ states for a tensor function. Depending on the functions defined to characterize these two parameters different solid performances can be obtained.

3 NEW ISOTROPIC HARDENING LAW

Equation (3) allow the incorporation of different hardening laws to describe the material performance. In the Barcelona model defined in [1], the laws defined are driven by the fracture energy of the material. This work presents a new law, specially developed for steel materials, that has been designed to reproduce their hardening and softening performance

under monotonic and cyclic loading conditions. This law also depends on the fracture energy of the material.

3.1 Fracture Energy

Classical fracture mechanics defines the fracture energy of a material as the energy that has to be dissipated to open a fracture in a unitary area of the material. This energy is defined as:

$$G_f = \frac{W_f}{A_f} \tag{4}$$

where W_f is the energy dissipated by the fracture at the end of the process, and A_f is the area of the surface fractured. The total fracture energy dissipated, W_f, in the fracture process can be used to define a fracture energy by unit volume, g_f, required in a continuum mechanics formulation:

$$W_f = G_f \cdot A_f \equiv \int_{V_f} g_f \, dV \tag{5}$$

This last equation allows establishing the relation between the fracture energy defined as a material property, G_f, and the maximum energy per unit volume:

$$g_f = \frac{W_f}{V_f} = \frac{W_f}{A_f \cdot l_f} = \frac{G_f}{l_f} \tag{6}$$

Thus, the fracture energy per unit volume is obtained as the fracture energy of the material divided by the fracture length. This fracture length corresponds to the distance, perpendicular to the fracture area, in which this fracture propagates.

In a real section, this length tends to be infinitesimal. However, in a finite element simulation, in which continuum mechanics is applied to a discrete medium, this length corresponds to the smallest value in which the structure is discretized: the length represented by a gauss point.

Threrefore, in order to have a finite element formulation consistent and mesh independent, it is necessary to define the hardening law in function of the fracture energy per unit volume ([1], [6]). This value is obtained from the fracture energy of the material, G_f, and the size of the finite element in which the structure is discretized.

3.2 Hardening Function and Hardening Internal Variable

The hardening function defines the stress of the material when it is in the non-linear range. There are many possible definitions that can be used for this function fulfilling equation (3). Among them, here it is proposed to use a function that describes the evolution of an equivalent uniaxial stress state, like the one shown in Figure 3.

This equivalent stress state shown in Figure 3 has been defined to match the uniaxial stress evolution described by most metallic materials. This curve is divided in two different regions. The first region is defined by curve fitting from a given set of equivalent stress-equivalent strain points. The curve used to fit the points is a polynomial of any given order defined using

the least squares method. The data given to define this region is expected to provide an increasing function, in order to obtain a good performance of the formulation when performing cyclic analysis.

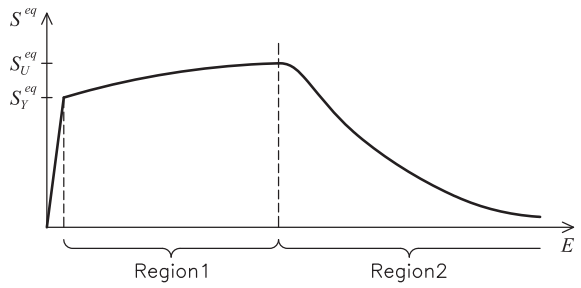

Figure 3. Evolution of the equivalent plastic stress

The second region is defined with an exponential function to simulate softening. The function starts with a null slope that becomes negative as the equivalent plastic strains increase. The exact geometry of this last region depends on the fracture energy of the material.

The hardening internal variable, κ^p, accounts for the evolution of the plastic hardening function, K. In current formulation κ^p is defined as a normalized scalar parameter that takes into account the amount of volumetric fracture energy dissipated by the material in the actual strain-stress state. This is:

$$\kappa^p = \frac{1}{g_f} \int_{t=0}^{t} S : \dot{E}^p dt \tag{7}$$

In the following figure is represented, shaded in green, the volumetric fracture energy required by a uniaxial material, for a given plastic strain E^p. The hardening internal variable defined in (7) is calculated normalizing this fracture energy by the total fracture energy of the system, g_f, which corresponds to the total area below the curve $S^{eq}(E^p)$, shaded with gray lines.

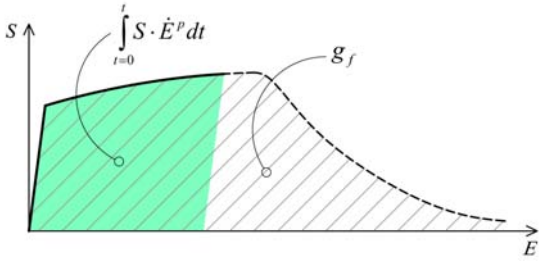

Figure 4. Representation of the volumetric fracture energy of a metallic material

Using the definition of the hardening internal variable defined in equation (7), it is possible to define the expression of the hardening function as:

$$K = S^{eq}(\kappa^p) \tag{8}$$

It can be easily proven that the hardening function and internal variable defined in equations (7) and (8) fulfill the rate equations (3). And the h_k and $h_{\mathbf{k}}$ functions defined in this expression become:

$$h_k = \frac{\partial S^{eq}}{\partial \kappa^p} \qquad h_{\mathrm{k}} = \frac{S}{g_t} \tag{9}$$

3.3 Expressions of the hardening function

In this section are provided the exact numerical expressions used to define the new hardening law presented in this work. This law is characterized with two different functions, each one defining the evolution of the equivalent stress in each region in which the equivalent stress performance is divided (see Figure 3).

Region 1: Curve fitting with polynomial

The first region is characterized with a polynomial defined by curved fitting from a given experimental data. Among the different available methods that can be used to define this polynomial, here is proposed to use the least squares method due its simplicity, computational cost, and good performance provided. The resultant relation between the stress and plastic strain in this region is:

$$S^{eq}(E^p) = a_0 + \sum_{i=1}^{N} a_i \cdot \left(E^p\right)^i \tag{10}$$

with N the order of the polynomial.

The volume fracture energy that is dissipated in this region can be obtained calculating the area below the $S^{eq} - E^p$ graph. This calculation provides the following value:

$$g_{t1} = \sum_{i=1}^{N+1} \frac{a_i}{i} \left(\left(E_2^p\right)^i - \left(E_1^p\right)^i \right) \tag{11}$$

being E_1^p and E_2^p the initial and final plastic strain values, respectively, that delimit the polynomial function region.

Although the equivalent plastic stress should depend on the plastic internal variable κ^p, in a cyclic simulation with isotropic hardening this approach will produce hysteresis loops with increasing stress amplitude (for a fixed strain amplitude). For this reason, current formulation calculates the equivalent plastic stress using the value of the equivalent plastic strain, which is calculated as:

$$E^p = \frac{S : E^p}{f(S)} \tag{12}$$

with $f(S)$ defined by the yield surface used to simulate the material, as it is shown in equation (1).

Finally, the derivative of the hardening function can be calculated with the following expression:

$$\frac{dS^{eq}}{d\kappa^p} = \frac{dS^{eq}}{dE^p} \cdot \frac{dE^p}{d\kappa^p} = g_t \cdot \frac{\sum_{i=1}^{N} i \cdot a_{i+1} \left(E^p\right)^{i-1}}{\sum_{i=1}^{N+1} a_i \left(E^p\right)^{i-1}} \tag{13}$$

Expression (13) is valid for values of κ^p that are comprehended between $\kappa_1^p = 0$ and $\kappa_2^p = g_{t1}/g_t$. The value of the upper limit of the internal variable shows that it is necessary define a value for the volumetric fracture energy of the material larger than g_{t1}. If the value defined is lower, the material will not be able to reach its ultimate stress as this will imply having a fracture internal variable larger than 1.0.

Region 2: Exponential softening

When the plastic internal variable reaches the volumetric plastic energy available in the first region: $\kappa^p = \kappa_2^p$. At this point isotropic hardening is defined by region two, which function is obtained with the following parameters:

1. The initial equivalent stress value is defined by the equivalent stress reached in the first region (S_2^{eq}). This value can be the one defined in the material characterization or can be a lower value if there has been some plastic energy dissipation in a cyclic process. In this last case, the value stress value has to be obtained from previous region.
2. The initial slope of the function is zero.
3. The volumetric fracture energy dissipated in this region is the remaining energy in the material: $g_{t2} = g_t - g_{t1}$

With these considerations in mind, the resultant equation that relates the equivalent stress with the plastic strain is:

$$S^{eq}(E^p) = S_2^{eq} \cdot \left[2 \cdot e^{-b \cdot \left(E^p - E_2^p\right)} - e^{-2b \cdot \left(E^p - E_2^p\right)}\right] \tag{14}$$

where $b = \dfrac{3 \cdot S_2^{eq}}{2 \cdot g_{t2}}$

The expression of the equivalent stress as a function of the hardening variable is obtained combining equation (14) and (7), obtaining:

$$S^{eq}(\kappa^p) = S_2^{eq} \cdot \chi \cdot \left(2 - \chi\right) \tag{15}$$

Being, $\chi = \sqrt{\frac{(\kappa^p - \kappa_2^p) \cdot 2b \cdot g_t}{S_2^{eq}} + 1}$

And the derivative of the hardening function is:

$$\frac{dS^{eq}}{d\kappa^p} = 2b \cdot g_t \cdot \left(\frac{1}{\chi} - 1 \right) \tag{16}$$

4 PERFORMANCE OF THE FORMULATION

In the following are included the results obtained from several simulations conducted to illustrate the performance of the formulation presented. These simulations can be divided in three different groups. The first group proves the ability of the formulation to characterize the mechanical performance of steel, under monotonic and cyclic loading conditions. The second set of simulations shows the performance of the developed formulation when it is used to characterize Ultra Low Cycle Fatigue. Finally, the third set of simulations intends to demonstrate the advantages of the approach proposed to simulate ULCF; this is done with the simulation of the steel response to a seismic-type load.

The main aim of all the simulations presented hereafter is to show the response obtained with the constitutive equation developed, and not to show the mechanical response of any particular structural element. Therefore, for the sake of simplicity, and to reduce the computational cost of the simulations, all of them have been conducted on a single hexahedral finite element. The element is fixed in one of its faces and the load is applied to the opposite face as an imposed displacement.

4.1 Simulation of the mechanical performance of steel under different loading conditions

To prove the ability of the model to simulate monotonic and cyclic tests made on steel, in the following are compared the results obtained from the numerical model with the results obtained from experimental tests performed by Universidade du Porto in the framework of the ULCF project. The tests were performed to a X52 steel.

The data used to define the numerical model has been obtained adjusting the solution of the model to the results of the experimental tests. To do so, it has been necessary to take into account that the effects of the kinematic and the isotropic hardening laws are coupled. This implies that the definition of the first region of isotropic hardening cannot be obtained from the experimental curve straightforward, as this curve does not take into account the displacement of the yield surface due to the kinematic hardening law. The most relevant parameters of the model are described in the following table.

Table 1. Mechanical properties of steel X52

Young Modulus	$2.05 \cdot 10^5$ MPa
Poisson Modulus	0.30
Elastic Stress (σ_Y^{eq})	270 MPa
Plastic Strain Softening (E_2^p)	27 %

C1 kinematic hardening	$5.0 \cdot 10^4$ MPa
C2 kinematic hardening	450
Fracture Energy	8.0 MN·m/m^2

In the following figures are included the stress-strain results obtained with the developed formulation for the material described. The green line corresponds to the numerical result and the red dots correspond to the experimental values provided by FEUP. Figure 5 shows the comparison made on a monotonic test. Figure 6 shows this comparison for two cyclic tests in which the sample is loaded with a fixed displacement oscillating between a tensile and a compressive strain of 0.5% and 1.5%.

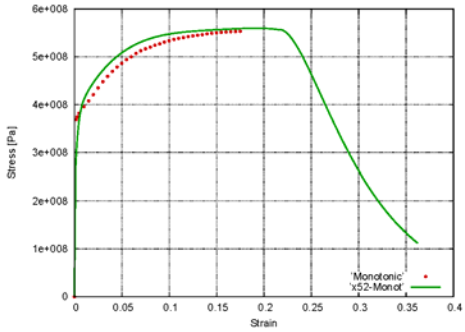

Figure 5. Comparison of numerical vs. experimental monotonic (a) and cyclic (b) test

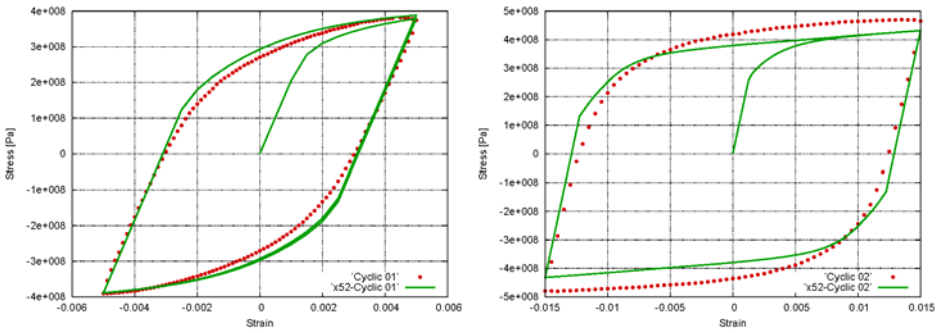

Figure 6. Comparison of numerical vs. experimental cyclic tests for a strain of 0.5% (a) and 1.5% (b)

Although the correspondence between the numerical and experimental results obtained for the different simulations is not perfect, it can be said that it is quite reasonable. Moreover if the discrepancy between the experimental tests is taken into account: while the numerical result is always the same, in Figure 5 and 6a the stress values seem over-predicted compared to the experimental ones and, in Figure 6b they seem to be under-predicted. This indicates that the experimental response obtained with the different specimens is not exactly the same, and that the numerical model provides a solution that is found between the limits of the experimental tests.

4.2 Simulation of Ultra Low Cycle Fatigue

Once having proved the ability of the model to characterize properly a x52 steel, this

section shows the performance of the formulation if it is used to characterize an ULCF failure. In the following figures is shown the response provided by the numerical model for a cyclic test. Figure 7a shows the stress-strain graph obtained for a simulation that is being loaded with 10 cycles. In this case all cycles follow the same stress-strain path. Figure 7b is represented the stress-strain response of the material when the simulation is extended to 30 cycles. This figure shows a reduction in the stress provided by the material for some cycles (the last ones). This stress reduction is consequence that the available hardening energy has been reached and that the material has started a softening process. We can consider that ULCF starts when this softening behavior starts.

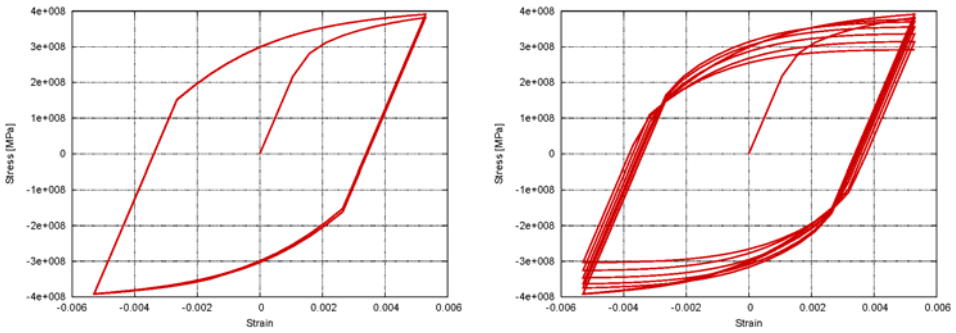

Figure 7. Response of the material during 10 cycles (a)-left, and during 30 cycles (b)-right

With this approach it is possible to obtain the material performance for different plastic strain amplitude cycles. The results obtained from these simulations are shown in Figure 8. This figure shows that the response of the material to ULCF presents a logarithmic variation, as it is expected according to what is described in literature and reported by several authors (such as Xue [1]).

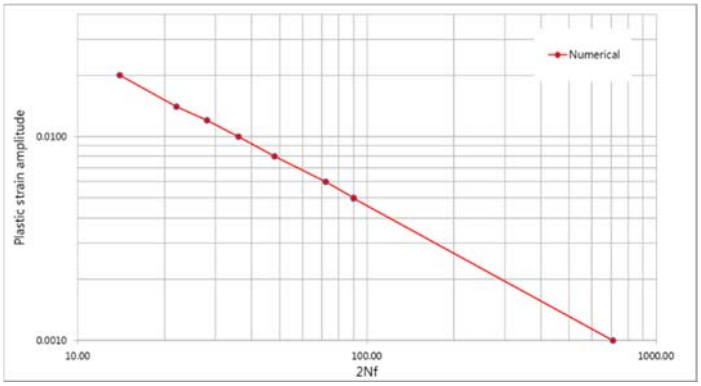

Figure 8. Number of cycles that can be applied to the material before ULCF failure

4.3 Advantages of the approach proposed

Previous results have shown that the proposed constitutive equation is capable of predicting material failure after applying several cycles to the material; it has shown also that the number of cycles depends on the plastic strain amplitude and, finally, that this is a logarithmic variation (as it was expected). However, these capabilities do not present major advantages compared to other approaches such as the Coffin-Manson rule, or any other

analytical expression capable of defining the maximum number of cycles that can be applied for a given plastic strain.

The main advantage of the proposed approach is that the prediction of ULCF failure does not depend on the plastic strain applied, but on the energy dissipated during the cyclic process. Therefore, it is possible to vary the plastic strain in the cycles applied to the structure and the constitutive model will be still capable of predicting the material failure.

This is proved in the following example, where an irregular load, in frequency and amplitude, is applied to the material (Figure 9a). This load will provide the stress-strain response plotted Figure 9b. As it can be seen, the load applied produces several loops, each one with a different plastic strain.

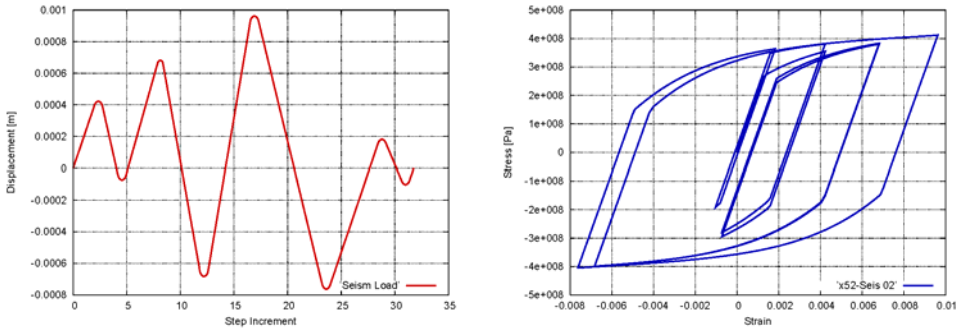

Figure 9. Seismic-type load applied (a) and material stress-strain response (b)

The model is capable of capturing the energy dissipated in each one of these loops and, therefore, to evaluate the fracture energy available in the material after having applied the load. In the following figure it is shown the response if a monotonic load is applied after two repetitions of the load depicted in Figure 9a. This response is superimposed with the response of a monotonic load. The result obtained shows that this two cycles have dissipated some energy and, therefore, the maximum strain reached by the model before failure is lower than the strain reached with the monotonic test.

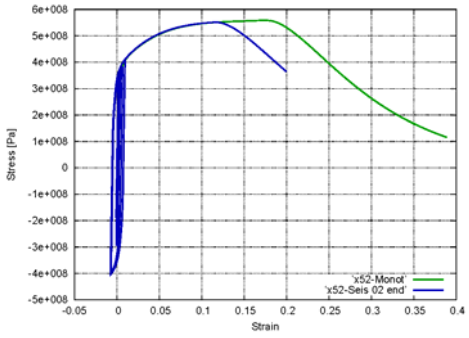

Figure 10. Response of the material after applying two seismic-type cycles

It is also possible to repeat several times the irregular load, shown in Figure 9a, to study the number of repetitions that are required to reach material failure. Figure 11 shows the stress-strain response of the material after twelve seismic-type cycles. This graph shows that in the last six cycles the stress developed by the material has been reduced, which allows to

conclude that the material can hold only six cycles of the load described.

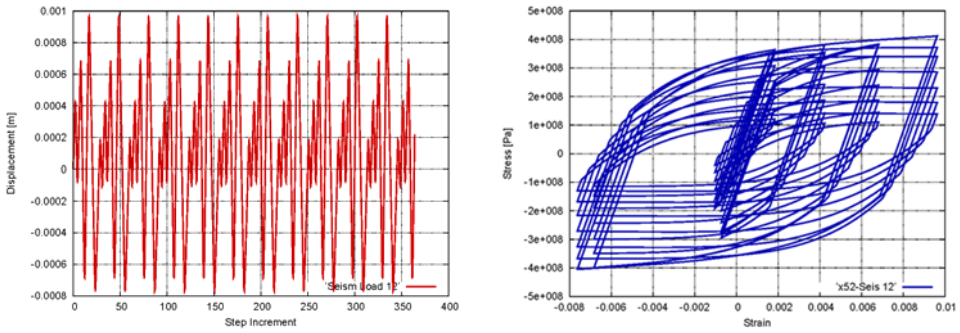

Figure 11. Response of the material after twelve seismic-type cycles

5 CONCLUSIONS

This document has presented a constitutive model to characterize the mechanical performance of steel, capable of taking into account the isotropic and kinematic hardening effects. The size of the yield surface is determined by the isotropic hardening law that depends on the amount of energy dissipated by the material.

Preliminary results, made on the material, show that the simulation of steel with the proposed approach is capable of capturing the effect of Ultra Low Cycle Fatigue in the material. Moreover, the model not only is capable of predicting the failure for a specific cyclic load, but it is also capable of predicting the material failure for cyclic irregular loads.

ACKNOWLEDGEMENTS

This work has been supported by the Research Fund for Coal and Steel through the ULCF project (RFSR-CT-2011-00029) and by the European Research Council under the Advanced Grant: ERC-2012-AdG 320815 COMP-DES-MAT "Advanced tools for computational design of engineering materials"

REFERENCES

[1] J. Lubliner, J. Oliver, S. Oller and E. Oñate. *A plastic-damage model for concrete*. International Journal of Solids and Structures, 25(3): 299-326 (1989)

[2] Lee, J. and Fenves, G. *Plastic-Damage Model for Cyclic Loading of Concrete Structures*. Journal of Engineering Mechanics, 124(8): 892–900. (1998)

[3] F.C. Campbell, *Elements of Metallurgy and Engineering Alloys*, ASM International, Ohio, USA (2008)

[4] L Xue, *A unified expression for low cycle fatigue and extremely low cycle fatigue and its implication for monotonic loading*, *Int. J. Fatigue*, 30, 1691-1698 (2008).

[5] B. Luccioni, S. Oller and R. Danesi. *Coupled plastic-damage model*. Computer Methods in Applied Mechanics and Engineering, 129: 81-90 (1996)

[6] S. Oller. *Fractura mecánica. Un enfoque global*. Centre Internacional de Mètodes Numèrics a l'Enginyeria (CIMNE). Barcelona, Spain, 2001. ISBN: 84-89925-76-3

[7] J. Lemaitre and J.-L. *Chaboche. Mechanics of Solid Materials*. Cambridge University Press. New York, USA, 1990